Multiple spin-flip Raman scattering in CdSe/ZnMnSe quantum dots

N. V. Kozyrev,* R. R. Akhmadullin, B. R. Namozov, Yu. G. Kusrayev, I. V. Sedova, S. V. Sorokin, and S. V. Ivanov
Ioffe Institute, St. Petersburg 194021, Russia

(Received 25 August 2018; revised manuscript received 7 December 2018; published 2 January 2019)

Multiple Mn^{2+} spin-flip Raman scattering (SFRS) in Voigt geometry was observed in self-organized disk-shaped quantum dots (QDs) of $CdSe/Zn_{0.99}Mn_{0.01}Se$, where magnetic ions and QD carriers are spatially separated and therefore the exchange interaction between them is expected to be weak. Many lines (about ten) were observed in SFRS spectra, yet the overlapping of the hole wave function with Mn^{2+} ions is very small, in agreement with both the absence of observable Zeeman splitting of the photoluminescence line and the calculation. Interesting polarization properties of SFRS spectra were observed which could be affected by tilting the sample out of normal alignment and changing the temperature. These polarization properties were attributed to the selection rules in SFRS in Voigt geometry. It has been found that the theoretical model suggested by Stühler *et al.* [J. Cryst. Growth **159**, 1001 (1996)] does not describe the SFRS spectra in systems with weak exchange interaction between charge carriers and magnetic ions. A qualitative model is suggested here for description of SFRS in such systems.

DOI: 10.1103/PhysRevB.99.035301

I. INTRODUCTION

Nowadays the search for and study of phenomena connected to a particle's spin degree of freedom are the actual problems in modern semiconductor physics. The materials which can be used to study these phenomena are the diluted magnetic semiconductors (DMSs). DMSs are $A^{II}B^{VI}$ ($A^{III}B^{V}$) alloys whose cation sublattice is partially substituted with magnetic transition metal ions such as Mn, Co, or Fe, e.g., CdMnTe and CdMnSe. The essential property of a DMS is the strong exchange interaction between charge carriers and magnetic ions, that brings a giant spin splitting of band states, which leads in its turn to some peculiar phenomena such as giant Faraday rotation [1,2] or magnetic polaron formation [3]. Nanostructures, such as quantum wells (QWs) or quantum dots (QDs), based on DMSs, deserve special attention because of the quantum confinement in these structures, that leads to a significant enhancement of all spin interactions in comparison to bulk materials [4]. In particular, it is easier to form the magnetic polaron in these quantum structures than in bulk materials [5].

An interesting effect of multiple-Mn^{2+} spin-flip Raman scattering (SFRS) can be observed in DMS-based nanostructures. It manifests itself as a large number of equally spaced lines in the spectrum of the resonant Raman light scattering, and it was first observed in quantum well (QW) CdMnTe/CdMgTe and reported by Stühler *et al.* [6]. A model of the SFRS in which coherent precession of the manganese ions' net spin takes place, was proposed therein. In this model the exciton plays the role of the intermediate state, and transfer of the energy and spin goes via this state. Therefore it has to be clarified that the direct optical transitions within the Mn^{2+} d shell ($^6A_1 \rightarrow {}^4T_1, {}^4T_2, {}^4A_1, {}^4E$, which are about 2.2 eV and higher), thoroughly described elsewhere [3], are out of the scope of this effect because these transitions are forbidden by the parity and spin, and are negligible compared to the exciton transitions.

This phenomenon itself is a matter of high interest and has been investigated in several papers. For example, in a recent paper [7] the authors report "fractional" SFRS peaks in CdMnTe/CdMgTe quantum wells. In [8] the number of SFRS lines in CdMnTe/CdMgTe QWs was investigated for dependence on the angle between growth axis and magnetic field. Also, in [9] the in-plane anisotropy of the heavy hole g factor was studied by means of SFRS measurements. In the paper [10] it was reported that multiple manganese SFRS (with number of lines >5) could also be observed in Faraday geometry, though the theory [6] predicted multiple SFRS only in Voigt geometry. We also refer the reader to papers [11,12] where the first results of experiments on SFRS in CdMnSe/ZnMnSe quantum dots were reported.

Besides the large number of scattering lines in CdMnTe/CdMgTe QWs, some interesting polarization properties of the SFRS spectra can be seen [13]. Namely, if the experiment is performed in parallel (crossed) linear polarizations of the incident and registered light, then intensities of the SFRS lines with even (odd) numbers will be damped. These polarization properties are claimed to be due to the selection rules for the SFRS, which cause them to appear in the Voigt configuration when the optical quantization axis and the magnetic field are perpendicular to each other. Although the theory suggested in [6] and improved in [13] was fairly consistent with the experimental results reported there, the universality of it is still under discussion, because it has not been applied to other systems and conditions.

One of the aims of our research was to verify the universality of the theoretical model [13] by applying it to the SFRS results obtained from self-organized CdSe/ZnMnSe QDs in the regime of the weak exchange interaction, where

*kozyrev.nikolay@bk.ru

magnetic ions are located in the barriers and exchange interaction between them and holes is weak to the extent of penetration of the holes' wave function into barriers. Another aim was to investigate the SFRS selection rules in this system. The experimental results show that, as was in case for QW CdMnTe [13], the selection rules predicted by the theory are partially broken. The situation gets "worse" when changing the angle between the growth axis and the magnetic field from 90°, and when decreasing the temperature. On the other hand, in the regime of the weak interaction between charge carriers and magnetic ions (implemented in the structure investigated in the current work), as we have shown below, the theory suggested in [13] predicts that there should be only few lines in the SFRS spectrum, which is in unresolvable contradiction with experiment. The possible explanation of this discrepancy could be found in an alternative mechanism of the multiple manganese spin-flip resonant Raman light scattering. We suggest a qualitative model of the phenomenon in which the transitions between spin sublevels of the magnetic ions are forced by the localized hole exchange field that is dynamically changing over time.

II. EXPERIMENT AND RESULTS

The structure under investigation was grown pseudomorphically by molecular-beam epitaxy (MBE) on a semi-insulated GaAs (001) substrate via a GaAs buffer epilayer. The CdSe QD sheet was grown by conventional MBE growth mode with a nominal thickness of ∼2 monolayers (MLs) and surrounded at bottom and top with $Zn_{0.99}Mn_{0.01}Se$ barriers with thicknesses of 60 and 20 nm, respectively. The whole structure was doped by chlorine donors to provide an average doping level of $n \approx 2 \times 10^{17}$ cm^{-3}.

The sample was contained in a bath cryostat on a movable sample holder with the possibility of turning the sample around the vertical axes by angle ϕ. The measurement of photoluminescence (PL) spectra under above-barrier excitation in the longitudinal magnetic field (Faraday geometry) is shown in Fig. 1. Two regions of PL are present in the PL spectra: one is near 2.8 eV, which corresponds to the PL from the ZnMnSe barrier, and another is a broad, strongly inhomogeneous PL line from QDs near 2.35 eV with a width of about 40 meV. The barrier PL manifests a giant Zeeman splitting in the 6 T field with a value of about 16 meV. This value corresponds to about 0.5% of Mn^{2+} ion molar concentration. On the other hand, the quantum dots' broad PL line splitting in a magnetic field up to 6 T can be estimated to be less than 0.5 meV, i.e., it is much less then the line width; no giant Zeeman splitting can be observed. This high contrast between Zeeman splitting values from barrier PL spectrum and QDs PL spectrum points to the fact that the samples' structure is as it was designed to be, and no sufficient manganese diffusion into QDs takes place. That is, the interaction between charge carriers localized in the QDs with the manganese ions situated in the barrier is too small to give the giant Zeeman splitting. Despite the smallness of Zeeman splitting at 6 T, there is some observable shift towards high energy of the PL line in the magnetic field. This shift has the same sign for σ^+ and σ^- and could be attributed to the diamagnetic shift. Although the PL Zeeman splitting is not observable, a circular polarization

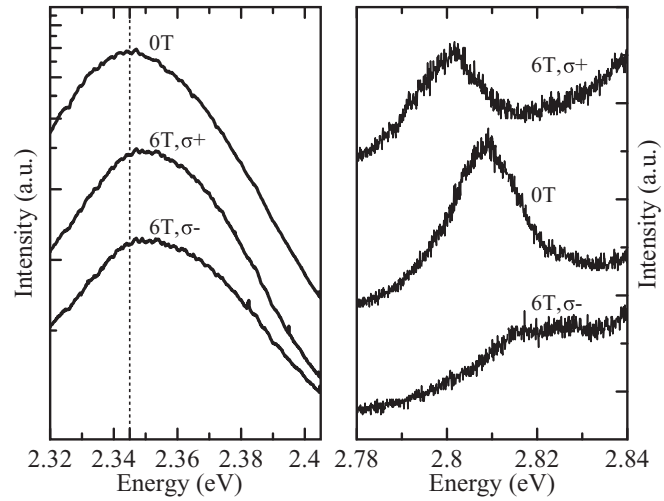

FIG. 1. The PL spectra at $T = 1.6$ K in $B = 0$ T and $B = 6$ T for σ^+ and σ^- polarization in Faraday mode obtained under above-barrier nonpolarized illumination from the CdSe QD layer (left panel, semilogarithmic scale) and from the ZnMnSe barrier (right panel, spectra are shifted for clarity). PL from the barrier exhibits a huge Zeeman splitting of about 16 meV at 6 T, which corresponds to about 0.5% amount of Mn^{2+} ions in the barrier. According to the spectra from the QDs only conventional Zeeman splitting (less than 0.5 meV, that corresponds to $g \leqslant 1.4$) can be observed in the magnetic field, but polarization of PL of about 40% occurs. The dashed vertical line on the right panel shows the 2.345 eV laser excitation energy used in SFRS

degree of PL about 40% is present. The numerical estimation of the circular polarization degree of the line splitting of 0.5 meV at temperature 1.6 K gives a value of nearly 100%, which can be lowered to 40% by increasing the temperature to about 10 K. This heating could have taken place in the experiment because of the quite large excitation power density (about 1 W/cm^2).

For the sake of sample characterization we measured the PL dynamics from the QDs at the 2.34 eV point [Figs. 2(a1) and 2(a2)]. The kinetics show an average fast characteristic decay time about 150 ps. This fast (less than 1 ns) PL dynamics observed in our case points to the fact that the exciton in the QD is a direct one, i.e., the CdSe/ZnMnSe QDs belong to the type-I structures. It is known that the indirect excitons in type-II heterostructures (where electrons and holes are spatially separated) have much longer lifetimes, which can exceed 100 ns [Fig. 2(b)]. Our observation is also supported by several papers wherein authors also report that CdSe and ZnSe have the type-I band structure alignment: e.g., [14] where the quantization levels and parameters of the ZnCdSe/ZnSe quantum wells were calculated and it was found that the band structure for the heavy holes is always type I; also similar structures with embedding of the CdSe/ZnSe nano-islands were studied in [15–17]. Together, the short exciton lifetime and very small Zeeman effect in the PL from the QDs shows that the excitons and manganese ions are spatially separated from each other and moreover are situated in different layers of the structure.

It is worth saying a few words about spectral linewidth and spectral position of the PL. Many articles have been published

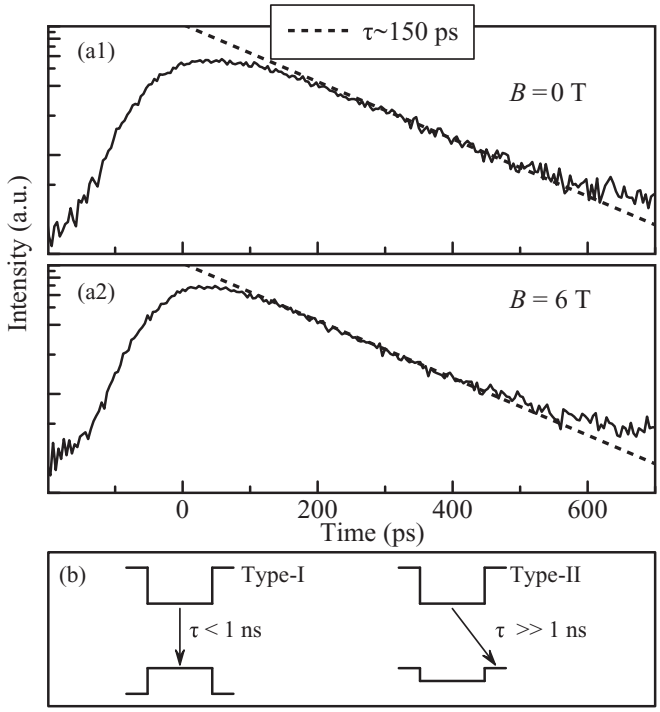

FIG. 2. PL dynamics (2.33 eV detection) in $B = 0$ T (a1) and in $B = 6$ T (a2) in semilogarithmic scale. The characteristic decay time of the PL is about 150 ps in both cases. The characteristic decay time of the excitation pulse is less than 50 ps. (b) representation of the different PL decay times for type-I and type-II heterostructures.

about sizes of self-organized CdSe/ZnSe QDs grown on a GaAs substrate estimated by TEM (e.g., [18–20]), and it has been shown that the lateral sizes (from ∼20 nm to ∼100 nm) of these quantum structures are much larger than the vertical ones (from ∼1 nm to ∼5 nm); therefore these QDs can be considered as quasi-two-dimensional objects. The linewidth of the PL is strongly inhomogeneously broadened due to the strong variation of QD size and, the PL spectral position is shifted from the bulk (∼1.75 eV) to 2.3 eV as a result of the quantum confinement. According to our estimations the vertical size of a QD should be ≈1.4 nm in order to have PL shifted by 0.55 eV. In these estimations the band gaps of the CdSe and ZnSe were taken as 1.75 and 2.82 eV respectively [21]. The valence band offset parameter was taken as 0.28 [21], therefore the quantum potential depths were taken as 0.3 and 0.77 eV for the valence band and the conduction band respectively.

The resonant SFRS experiment was performed in the Voigt backscattering geometry with crossed $(-z\sigma\pi z)$ and parallel $(-z\sigma\sigma z)$ configurations of incident and detected light polarization planes in an external magnetic field $B = 6$ T and at different temperatures $T = 1.6$ K, $T = 10$ K, $T = 20$ K. Here σ means that the light polarization vector is perpendicular to the magnetic field, and π means that they are parallel to each other. An argon laser was used as the light source, with a photon energy of 2.345 eV, which overlaps the PL spectrum of QD ensemble. As mentioned before, the PL spectral broadening is due to the spreading of sizes, thus by exciting with a spectrally narrow laser line with a specific

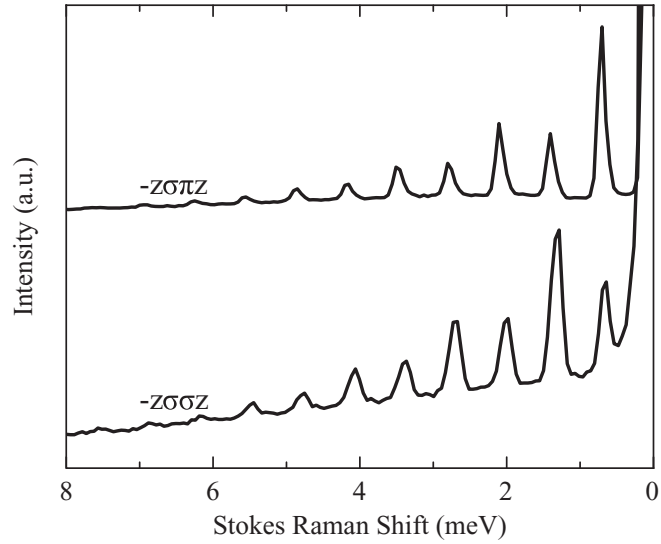

FIG. 3. SFRS spectra in crossed and parallel polarization in $T = 1.6$ K and $B = 6$ T measured in the backscattering Voigt geometry. Up to 11 peaks can bee seen. Spectra are shifted for clarity.

wavelength we selectively excite QDs with only one particular vertical size, which is 1.4 nm for the 2.345 eV laser energy.

Figure 3 shows the SFRS spectra in $B_{\text{ext}} = 6$ T and at $T = 1.6$ K in two configurations, where up to 11 narrow scattered light lines can be seen. The difference between positions of the lines gives us the manganese g-factor value equal to 1.97 ± 0.01. This value is close to $g = 2.00$ which was obtained by the electron paramagnetic resonance (EPR) technique on $A^{II}B^{VI}$: Mn DMSs [22]. Many lines in the SFRS spectra can be explained by the process of multiple Mn^{2+} transition between spin sublevels, which will be described later. The SFRS picture exhibits polarization properties varying in different experimental configurations: for crossed (parallel) polarizations even (odd) scattering lines are damped. As mentioned in the Introduction, these properties were first observed in [13] by Stühler *et al.*, who claimed that these polarization properties of SFRS are due to the selection rules. These selection rules say that the even (odd) numbered SFRS lines will be totally absent in the Voigt backscattering geometry with crossed (parallel) polarization planes of the incident and scattered light. However, as shown in [13] and as we observed, these selection rules are partially broken: in both configurations the absence of corresponding lines is not absolute. Stühler *et al.* claimed that this partial breaking of these selection rules is essentially because of the splitting of the heavy-hole states. This splitting was said to be occurring from the undulations of the quantum structure interfaces [13]. We would like to complement that statement with the several assumptions. The splitting of heavy hole states also can appear, first of all, from the magnetic-induced mixture between heavy hole and light hole states in the magnetic field, and, secondly, from the fact that the heavy hole has a small yet nonzero in-plane g factor owing to the in-plane anisotropy of the QDs [9].

This polarization behavior changes by turning the sample and thus changing the angle between the sample growth axis and the magnetic field. In order to determine the angular dependence of SFRS spectra, we slightly changed the

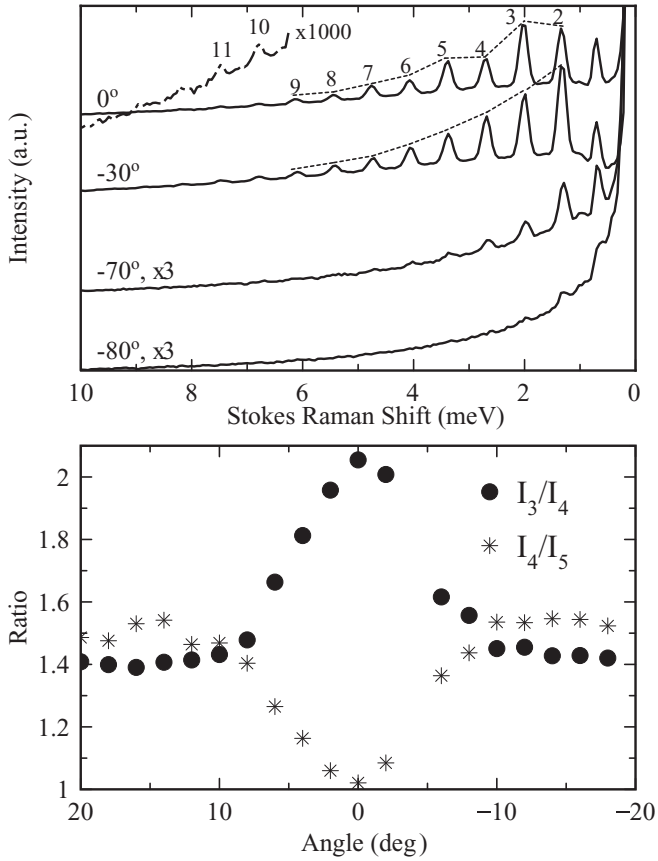

FIG. 4. Upper panel shows $(-z\sigma\pi z)$ configuration SFRS spectra measured in different angles between normal to the external magnetic field and growth axis of the sample. The first peak is damped by the bandpass function of the Raman spectrometer. $B = 6$ T, $T = 1.6$ K. On the lower panel the dependence of the intensity ratio between odd and even numbered neighbor SFRS peaks on the angle is shown.

experimental setup and added a bandpass filter to our Raman spectrometer. After this procedure the first SFRS line became damped and we did not use it in the consideration. The upper panel of the Fig. 4 shows the SFRS spectra measured at different tilting angles and represents this "depolarization" of SFRS: by turning the sample out of the normal alignment, the intensity damping of the SFRS lines with even numbers in $(-z\sigma\pi z)$ configuration decreased. After 80° of tilting angle the SFRS lines vanish. The lower panel of the Fig. 4 shows the dependence of the intensity ratio between odd and even numbered neighbor SFRS lines on the angle ϕ. After tilting of the sample by $\phi \approx 10°$ the selection rules are fully broken. That follows from the fact that the ratios between odd and even SFRS peaks stop depending on the angle during further tilting of the sample. In normal alignment of the sample this polarization picture is clearly seen at all temperatures from 1.6 to 30 K. On the one hand, with increasing temperature a general decrease of the SFRS intensity occurs, which can be seen in Fig. 5. On the other hand the selection rules are getting "better": intensities of the peaks with even number become more damped with increasing temperature. As one can see in the inset of Fig. 5, the ratio between intensities of the neighbor SFRS peaks changes monotonically.

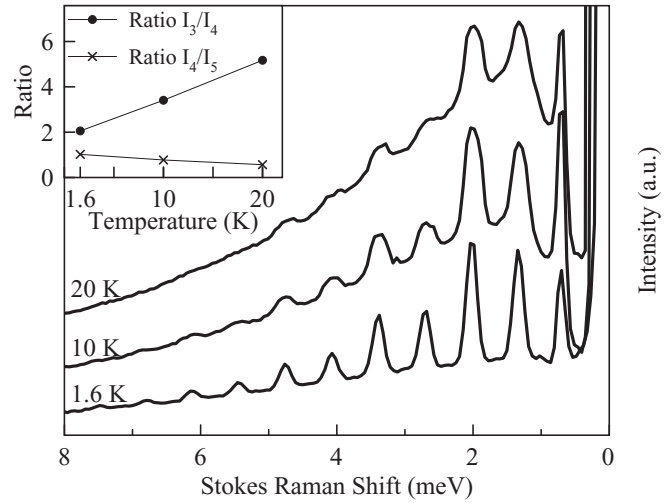

FIG. 5. $(-z\sigma\pi z)$ configuration SFRS spectra measured in normal alignment of the sample at different temperatures $T = 1.6$ K, $T = 10$ K, $T = 20$ K, and in the magnetic field $B = 6$ T. The inset shows the ratio between intensities of the neighbor SFRS lines: the third peak intensity to the fourth peak intensity (circles) and the fourth peak intensity to the fifth peak intensity (crosses). The spectra were shifted for clarity.

III. DISCUSSION

The Raman scattering process as a resonance effect includes an intermediate state creation; an exciton in our case. Via this state an energy can be transferred between the photon and the object on which it is scattering. Due to the quantum confinement, a heavy hole spin in an ideal two-dimensional structure is aligned to the sample growth axis and does not precess in the in-plane external magnetic field (the in-plane g factor is zero). Therefore Mn^{2+} ions which are in the localization area of that exciton feel the exchange field $\mathbf{B}_{\text{exch}}$ of the photoexcited heavy hole during the intermediate state lifetime. Hence the magnetic moment of those Mn^{2+} precesses in total magnetic field $\mathbf{B}_{\text{total}}$ which is the sum of the exchange $\mathbf{B}_{\text{exch}}$ and the external $\mathbf{B}_{\text{ext}}$ magnetic fields (Fig. 6), and the change of the magnetization projection on the $\mathbf{B}_{\text{ext}}$

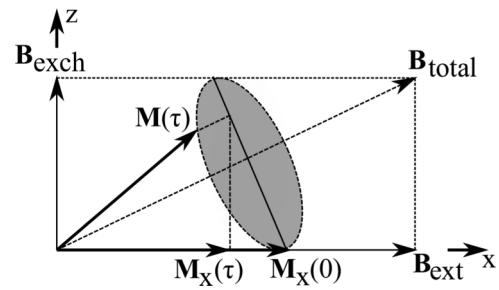

FIG. 6. Graphical representation of the multi-spin-flip Raman scattering effect. At $t = 0$, net magnetization of Mn^{2+} ions had a projection on $\mathbf{B}_{\text{ext}}$. After the exciton creation, this net magnetization starts to precess around the $\mathbf{B}_{\text{total}}$ and by the time τ, when the exciton recombines, net magnetization has a different projection on the external magnetic field. Therefore $M_x(0) - M_x(\tau)$ shows how many Mn^{2+} ions experienced a transition between spin sublevels.

axis leads to the collective multiple spin flips of Mn^{2+} ions. Many lines in SFRS spectra due to this mechanism were first observed and described in [6] and [13]. In the latter, as mentioned in the Introduction, the model of multi-spin-flip Raman scattering had been suggested in order to describe the polarization properties exhibited in the SFRS spectra, and that model was successfully applied to describe experiments on CdMnTe quantum wells. We used the theory proposed there in attempts to study the SFRS and the selection rules in the case where the interaction between Mn^{2+} and holes is defined by the penetration of the latter into the magnetic barriers. For more details of that process one can take a look in that articles and references therein.

To calculate the intensity of the scattering peak of number n depending on the lifetime of the intermediate state involved in the scattering process, the following formula was suggested in [13]:

$$I_n = \frac{1}{\tau}\underbrace{\int_{-\pi}^{\pi} d\theta\, G(\theta)}_{\text{part 3}} \int_0^{\infty} dt \overbrace{\left|\tfrac{1}{2}(1 \pm (-1)^n e^{i\Delta E(\theta)t/\hbar})\right|^2}^{\text{part 2}} \times \underbrace{e^{-t/\tau}\frac{N(t)^n}{n!}e^{-N(t)}}_{\text{part 1}}. \quad (1)$$

This formula can be divided into three parts. *Part 1* represents the main core of the formula describing the multi-spin-flip Raman scattering process based on the probability of several Mn^{2+} spins transition during the lifetime τ of that intermediate state. $N(t)$ is the change of the Mn^{2+} net spin projection on $\mathbf{B}_{\text{ext}}$ during the precession around $\mathbf{B}_{\text{total}}$, and has the following form:

$$N(t) = \int_V n_{Mn}\langle S\rangle(B_{\text{ext}}, T)\sin^2(\delta)[1 - \cos(\omega_L t)]dV, \quad (2)$$

where the integral is taken over the volume of the exciton V; n_{Mn} is the density of Mn^{2+} ions in the QDs; δ is the angle between $\mathbf{B}_{\text{total}}$ and $\mathbf{B}_{\text{ext}}$; $\langle S\rangle(B_{\text{ext}}, T)$ is the mean expectation value of the Mn^{2+} spin in the external magnetic field at a given temperature T, and it is described by the Brillouin function (e.g., [3]); and ω_L is the Larmor frequency for the Mn^{2+} spin in $\mathbf{B}_{\text{total}}$. The hole exchange magnetic field is defined as the following:

$$B_{\text{exch}}(\vec{r}) = \frac{\beta|\psi(\vec{r})|^2 J}{3\mu_B g_{\text{Mn}}}, \quad (3)$$

where β is the exchange constant between the Mn^{2+} ion and the hole, μ_B is Bohr's magneton, g_{Mn} is the manganese g factor, and J is the spin of the heavy hole. $\psi(\vec{r})$ is the hole wave function. We are interested only in that part of the wave function which penetrates into the magnetic ZnMnSe barriers. The sample under investigation has a layer of self-organized disk-shaped quantum dots with lateral sizes significantly larger than their vertical sizes, and moreover they are larger than the exciton radius in CdSe (~5 nm), so we can estimate the penetration of the hole wave function into barriers as if it was a conventional two-dimensional quantum well confined in the $\vec{z}$ direction. Along the $\vec{x}$ and $\vec{y}$ directions this structure does not have any confinement and we put the density of probability in these directions as the area of the circle with the radius the same as that of the exciton: $|\psi_{xy}|^2 = \frac{1}{\pi r_{\text{exc}}^2}$. Therefore, using the depth of the QW energetic potential for the holes as 0.3 eV, the width of the QW as 1.4 nm, the effective mass of heavy hole as $0.45m_0$, and exciton radius as 5 nm, we obtain the picture of the hole exchange field distribution (Fig. 7). One can see that the exchange magnetic field of the hole in such a quantum structure could reach very high values which are comparable to that of the external magnetic field. However, on the border of the QD its value drops to the 0.85 T and then exponentially decays with increasing distance from the QD.

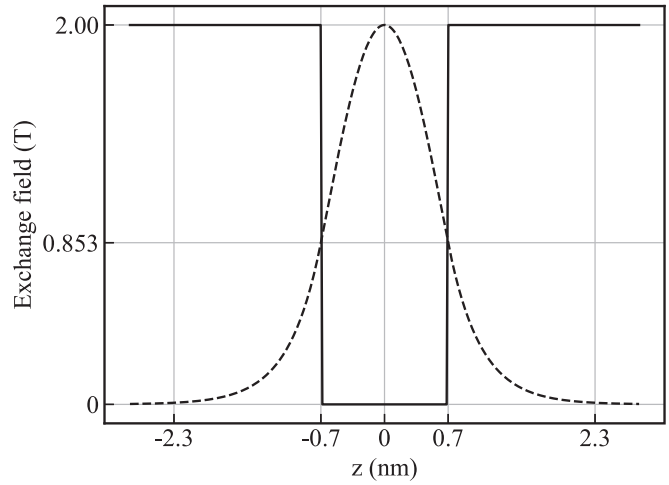

FIG. 7. The spatial distribution of exchange magnetic field (dashed line) and energetic profile of the QD (solid line) along the $\vec{z}$ direction. The maximum exchange magnetic field is in the center of the QD and reaches ~2 T; the magnetic field on the QD's borders is ~0.85 T. 2.3 nm is the point which surrounds 99% of the heavy hole wave function localization.

Taking into account the fact that δ (the angle between $\mathbf{B}_{\text{ext}}$ and $\mathbf{B}_{\text{total}}$) and the Larmor frequency precession around $\mathbf{B}_{\text{total}}$ depend on z, one can then modify Eq. (2) into the following form:

$$N(t) = \pi r_{\text{exc}}^2 n_{Mn}\langle S\rangle(B_{\text{ext}}, T) \times 2\int_{a/2}^{\infty} \sin^2[\delta(z)]\{1 - \cos[\omega_L(z)t]\}dz. \quad (4)$$

Here the factor 2 before the integral means that the penetration from both sides of the QD is the same.

Part 2 of formula (1) describes the selection rules. An ideal situation of a two-dimensional structure with perfect surface quality and normal alignment of the sample in Voigt backscattering geometry should have the simple form $|\frac{1}{2}[1 \pm (-1)^n]|^2$, where sign depends on the experiment configuration: minus (plus) stands for crossed (parallel) polarizations of the incident and detected light. The factor $e^{i\Delta E(\theta)t/\hbar}$ is added to represent the partial breaking of these selection rules. Essentially, it means that the presence of the heavy hole splitting in a magnetic field in Voigt geometry leads to the breaking of the selection rules. If the in-plane g factor of the heavy hole equals zero and the growth axis is perpendicular to the external magnetic field, the splitting

of the heavy hole is zero as well, and the selection rules will be fulfilled. The dependence of the heavy hole splitting on the angle means that the tilt of the sample growth axis by angle θ leads to the photoexcited hole spin not being perpendicular to $\mathbf{B}_{\text{ext}}$, and so the hole will have a nonzero projection on the external magnetic field axes. Thus the heavy hole state will be split into spin sublevels as $\Delta E(\theta) = \beta N_0 x_{Mn} S B_{5/2}(\mu_B g_{Mn} B_{\text{ext}} \sin(\theta)/kT)$. Here $B_{5/2}(x)$ is the Brillouin function and k is the Boltzmann constant.

As noted earlier, in [13] it was suggested that in the case where a perfect situation with flat interfaces of the quantum structure is not realized and some lowering of symmetry is present, the selection rules will be broken even in the perfect alignment of the sample. Undulations or skewness can be candidates for this lowering of symmetry. So it is necessary to take into account the angle distribution of these undulations or skewness. In our case we have only partial acceptance of the proposed selection rules, thus we made an assumption that our QDs have the mentioned skewness according to the suggestion. The integral in *part 3* contains the angular distribution function $G(\theta)$, which we take in the form of simple Gaussian,

$$G(\theta) = \frac{1}{\sqrt{2\pi\sigma^2}} e^{-\frac{(\theta-\phi)^2}{2\sigma^2}}, \tag{5}$$

where ϕ is the angle between sample growth axis and the magnetic field (in normal alignment it is 0°), and σ is the standard deviation representing the mean angular dispersion of the undulations. This part has an interplay with *part 2* because the integration over angles involves the depolarization factor as well.

We have used this formula for our case with the following parameters: $\tau = 1$ ps, $r_{\text{exc}} = 5$ nm, vertical size of the QD is 1.4 nm and its energetic depth is 0.3 eV for the valence band, $T = 1.6$ K, and $\sigma = 0.5°$. Taking into account only the part of the hole wave function situated in the barrier (the regime of weak exchange interaction), we have found that according to the theory there should be only few SFRS lines (crosses in Fig. 8), while we see in experiment many of them (diamonds in Fig. 8). On the other hand if we assume that a significant amount of the manganese ions are contained in the QDs themselves, the calculation would have given a SFRS spectrum consisting of many lines and their nonmonotonical behavior would be connected to the selection rules (dots in Fig. 8). Although this assumption could lead to a satisfactory matching between the experiment and the calculation, it is refuted by the fact that in the PL spectra in a magnetic field there is less than 0.5 meV Zeeman splitting. According to our estimations, if the manganese ions were in the QDs it would lead to a Zeeman splitting of the PL line of from 5 to 10 meV. Thus the QDs do not contain any significant amount of manganese and therefore the system under investigation is in the regime of the weak exchange interaction between the magnetic ions and the charge carriers. Referring again to Fig. 8, we come to the contradiction between the existing theory [13] and the experimental data obtained in the system with the weak exchange interaction regime.

In fact one looks at Eq. (4), representing the change of the manganese full spin projection on the external magnetic field direction, one can see that it follows a periodic law with a

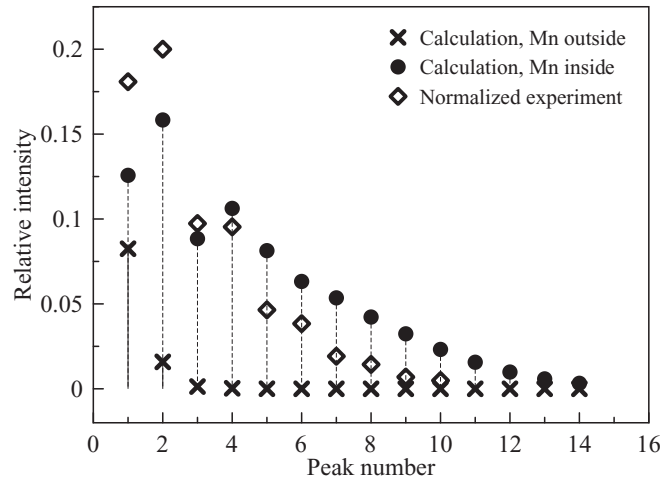

FIG. 8. Calculation of the theory [13] for the hole exchange field shown in Fig. 7. Circles are for Mn inside the QDs; crosses are for the Mn outside the QDs (weak exchange interaction regime). The diamonds are the normalized experiment data taken in normal alignment of the sample, at $T = 1.6$ K and in $B = 6$ T.

Larmor precession period and with the amplitude $N_{\max}$, which is the full possible change of Mn^{2+} net spin projection, and it defines how many spins could flip during the process of scattering. Therefore one can estimate the possible change of spin projection during the time τ for the cases where Mn^{2+} is inside and outside of the QDs. For the case where manganese is inside the QDs, $N_{\max} \approx 10$, and, for our case when manganese is outside, $N_{\max} \approx 0.5$. These two values are incompatible, and the latter indicates directly that in the system under investigation there should be only few spin-flips of Mn^{2+}.

In order to describe the SFRS phenomenon in systems with weak exchange interaction, we have an idea to suggest. The hole exchange field which influences on the Mn^{2+} spins could be considered as a pulse with the width of the intermediate state lifetime (∼1 ps) and the amplitude of the exchange field value (∼1 T). This exchange pulse could be Fourier transformed and represented as a sum of sinus functions with different frequencies and amplitudes. On the amplitude-frequency spectrum (AFS) one can find a frequency corresponding to that of the Mn^{2+} spin Larmor precession. Taking the integral of the AFS in the vicinity of that frequency, one can obtain the value of the amplitude of the exchange field. The integration range can be taken as a 1 GHz area close to the Larmor frequency, which corresponds to the characteristic time of the transverse relaxation of the manganese spin. Thus the amplitude at 177 GHz frequency (corresponding to the Larmor frequency in $B = 6$ T), is about 5 G (5×10^{-4} T). This value consists of the magnetic field strength value of the microwave field used in the EPR technique. The value is high enough to excite the transitions between spin sublevels of many manganese ions in EPR. Therefore we would like to note that this model of dynamical exchange field analogous to the EPR could be a clue for solving the riddle of the many SFRS lines in systems where the exchange interaction between magnetic ions and charge carriers is weak. This simple model describes the general dependencies of the

observed phenomenon. First of all, the number of the SFRS lines in the spectrum essentially depends on the number of manganese ions in the localization area of an exciton, rather than on the maximum possible change of the manganese net spin projection on the external magnetic field $N_{\max}$ (as in the theory of Ref. [13]). The second point follows by the general assumption that with increasing temperature all processes get faster. If one increases the temperature the lifetime of the intermediate state should decrease. That will lead to the decrease of the spectral density of the exchange field on the manganese paramagnetic resonance frequency, which in turn will lead to the decrease of the SFRS intensity.

In conclusion, we observed 11 SFRS lines in CdSe/ZnMnSe QDs in the regime of the weak exchange coupling between heavy holes and magnetic ions. We have found that the theoretical model suggested in [13] does not describe the SFRS effect in systems in that regime. This raises new questions not only about the resonant spin-flip Raman scattering phenomenon itself but also how the selection rules are to be included in the description of the SFRS. In an attempt to clarify the situation, a qualitative model of the dynamic exchange field has been proposed here instead.

ACKNOWLEDGMENTS

Yu.G.K., B.R.N., and R.R.A. thank the Russian Science Foundation for support of this work via Grant No. 18-12-00352. N.V.K. thanks the Russian Foundation for Basic Research for partial support of this work via Grant No. 15-52-12017 NNIO-a. I.V.S., S.V.S., and S.V.I. thank the Russian Foundation for Basic Research for "growth of system under investigation" support via Grant No. 15-52-12014 NNIO-a. We also thank K. V. Kavokin for fruitful discussions and I. I. Reshina who inspired the SFRS study in semimagnetic quantum dots and performed the first experiments.

[1] J. A. Gaj, R. R. Gałazka, and M. Nawrocki, Solid State Commun. **25**, 193 (1978).
[2] A. V. Komarov, S. M. Ryabchenko, O. V. Terletskii, I. I. Zheru, and R. D. Ivanchuk, Zh. Eksp. Teor. Fiz. **73**, 608 (1977) [Sov. Phys.—JETP **46**, 318 (1977)].
[3] J. K. Furdyna, J. Appl. Phys. **64**, R29 (1988).
[4] J. A. Gaj and J. Kossut, *Introduction to the Physics of Diluted Magnetic Semiconductors*, Springer Series in Materials Science Vol. 144 (Springer, Berlin, 2011).
[5] S. M. Ryabchenko and Yu. G. Semenov, Fiz. Tverd. Tela (Leningrad) **26**, 3347 (1984) [Sov. Phys. Solid State **26**, 2011 (1984)].
[6] J. Stühler, G. Schaack, M. Dahl, A. Waag, G. Landwehr, K. V. Kavokin, and I. A. Merkulov, Phys. Rev. Lett. **74**, 2567 (1995).
[7] A. V. Koudinov, A. Knapp, G. Karczewski, and J. Geurts, Phys. Rev. B **96**, 241303 (2017).
[8] L. C. Smith, J. J. Davies, D. Wolverson, M. Lentze, J. Geurts, T. Wojtowicz, and G. Karczewski, Phys. Rev. B **77**, 115341 (2008).
[9] A. V. Koudinov, Y. G. Kusrayev, B. P. Zakharchenya, D. Wolverson, J. J. Davies, T. Wojtowicz, G. Karczewski, and J. Kossut, Phys. Rev. B **67**, 115304 (2003).
[10] M. Byszewski, D. Plantier, M. L. Sadowski, M. Potemski, A. Sachrajda, Z. Wilamowski, and G. Karczewski, Physica E **22**, 652 (2004).
[11] I. I. Reshina, S. V. Ivanov, D. N. Mirlin, A. A. Toropov, A. Waag, and G. Landwehr, Phys. Rev. B **64**, 035303 (2001).
[12] I. I. Reshina, S. V. Ivanov, D. N. Mirlin, A. A. Toropov, A. Waag, and G. Landwehr, Phys. Status Solidi (b) **229**, 685 (2002).
[13] J. Stühler, G. Schaack, M. Dahl, A. Waag, G. Landwehr, K. V. Kavokin, and I. A. Merkulov, J. Cryst. Growth **159**, 1001 (1996).
[14] M. Maksimov, I. Krestnikov, S. Ivanov, N. Ledentsov, and S. Sorokin, Semiconductors **31**, 800 (1997).
[15] F. Gindele, U. Woggon, W. Langbein, J. M. Hvam, K. Leonardi, D. Hommel, and H. Selke, Phys. Rev. B **60**, 8773 (1999).
[16] C. Guenaud, E. Deleporte, A. Filoramo, P. Lelong, C. Delalande, C. Morhain, E. Tournie, and J. Faurie, J. Appl. Phys. **87**, 1863 (2000).
[17] P. Reiss, J. Bleuse, and A. Pron, Nano Lett. **2**, 781 (2002).
[18] N. Peranio, A. Rosenauer, D. Gerthsen, S. V. Sorokin, I. V. Sedova, and S. V. Ivanov, Phys. Rev. B **61**, 16015 (2000).
[19] S. V. Ivanov, A. A. Toropov, S. V. Sorokin, T. V. Shubina, I. V. Sedova, A. A. Sitnikova, P. S. Kop'ev, Z. I. Alferov, H.-J. Lugauer, G. Reuscher *et al.*, Appl. Phys. Lett. **74**, 498 (1999).
[20] D. Schikora, S. Schwedhelm, D. J. As, K. Lischka, D. Litvinov, A. Rosenauer, D. Gerthsen, M. Strassburg, A. Hoffmann, and D. Bimberg, Appl. Phys. Lett. **76**, 418 (2000).
[21] S. Adachi, *Properties of Semiconductor Alloys: Group-IV, III-V and II-VI Semiconductors*, Wiley Series in Materials for Electronic & Optoelectronic Applications Vol. 28 (John Wiley & Sons, New York, 2009).
[22] J. Lambe and C. Kikuchi, Phys. Rev. **119**, 1256 (1960).